$LiNMe_2$/THF slurry resulted in an initially green solution that ultimately turned yellow. The yellow solution was stirred for 12 h at room temperature to ensure reaction completion. The solvent was then removed in vacuo to give a pale yellow solid, which was purified by sublimation (120 °C, 10^{-4} Torr), yielding 0.23 g (73% based on tungsten) of $W_2(NMe_2)_6$. Anal. Calcd for $W_2C_{12}H_{36}N_6$: C, 22.78; H, 5.74; N, 13.34. Found: C, 22.53; H, 5.51; N, 13.02.

One-Pot Synthesis of $W_2(NMe_2)_6$. A 1-L three-neck flask was charged with WCl_4 (36.6 g, 112 mmol) and cooled to 0 °C, and THF (ca. 350 mL) was added via cannula. Sodium amalgam (1.0 wt.% Na, 112 mmol) was slowly added over a 90-min period by using a pressure-equalized dropping funnel. The solution was then warmed to room temperature and magnetically stirred for 3 h, resulting in a deep green color. The reaction flask was then cooled to 0 °C, and 3 equiv (based on WCl_4) of $LiNMe_2$ (17.1 g, 336 mmol) was added slowly (2 h) by using a solids-addition tube. The solution slowly turned from green to yellow-brown upon addition of $LiNMe_2$. After all the $LiNMe_2$ was added, the solution was warmed to room temperature, magnetically stirred for 12 h, and filtered through Celite, by cannula transfer, into a one-neck 1-L flask. The original reaction flask and the Celite pad were washed with THF (2 × 75 mL) to ensure complete product extraction. The solvent was removed in vacuo, leaving a brown solid which, upon sublimation (120 °C, 10^{-4} Torr), yielded bright yellow $W_2(NMe_2)_6$ (26.4 g, 75% based on WCl_4). The first isolated fraction (i.e., the first 10%) is occasionally contaminated with small quantities of $W(NMe_2)_6$.

Preparation of $W_2(O\text{-}t\text{-}Bu)_6$. In a Schlenk flask, $LiO\text{-}t\text{-}Bu$ (0.24 g, 3.0 mmol) was dissolved in 10 mL of THF, and the solution was cooled to 0 °C. By means of a solids-addition tube, $NaW_2Cl_7(THF)_5$ (0.50 g, 0.50 mmol) was added, and the solution was stirred at room temperature for 12 h. The solvent was removed in vacuo, producing a red solid. Hexane was added, and the solution was filtered through Celite in an attempt to remove LiCl. Removal of solvent in vacuo produced 0.27 g of a crude red solid. Recrystallization from hexane gave red needles of $W_2(O\text{-}t\text{-}Bu)_6$ (0.21 g, 52% based on tungsten), which were isolated by filtration. However, a satisfactory elemental analysis was not obtained. For a satisfactory elemental analysis of $W_2(O\text{-}t\text{-}Bu)_6$ prepared from $W_2(NMe_2)_6$ see ref 6.

Preparation of $W_2(CH_2\text{-}t\text{-}Bu)_6$. In a Schlenk flask, $LiCH_2\text{-}t\text{-}Bu$ (0.23 g, 3.0 mmol) was dissolved in 10 mL of THF, and the pale yellow solution was cooled to 0 °C. $NaW_2Cl_7(THF)_5$ (0.50 g, 0.50 mmol) was slowly added (10 min) via a solids-addition tube, and the mixture was stirred for 12 h at room temperature, resulting in an orange-yellow solution. Removal of solvent in vacuo yielded an orange solid, which was purified by sublimation (120 °C, 10^{-4} Torr) to give 0.22 g of $W_2(CH_2\text{-}t\text{-}Bu)_6$ (55% yield based on tungsten). ^1H NMR (23 °C, C_6D_6): δ 1.24 (CH_2CMe_3, s, 9 H), 2.52 (CH_2CMe_3, s, 2 H, $^2J_{^{183}W-^1H} = 10$ Hz). $^{13}C\{^1H\}$ NMR (23 °C, C_6D_6): δ 105.2 (CH_2CMe_3, $^1J_{^{183}W-^{13}C} = 91.4$ Hz), 35.0 (CH_2CMe_3), 34.2 (CH_2CMe_3). Anal. Calcd for $W_2C_{30}H_{66}$: C, 45.36; H, 8.32. Found: C, 45.24; H, 8.19.

Crystallographic Studies. The sample was handled by using previously described procedures.[20] An irregularly shaped crystal, approximately 0.10 × 0.12 × 0.18 mm, was selected for study. There were no prominent faces to facilitate accurate crystal measurement for absorption correction, so none was made. The crystal was mounted by using silicone grease and was transferred to the goniostat, where it was cooled to −151 °C for characterization and data collection. After eliminating a few diffraction maxima as being erroneous, the space group was identified as $P2_1/c$. The quality of the data appeared good. Four standards, measured every 300 data, showed no systematic trends. The averaging for 504 redundant data had a residual of 0.037.

The structure was solved by a combination of direct method (MULTAN78) and Fourier techniques. No attempt was made to find hydrogens from the difference map. After anisotropic refinement of all non-hydrogen atoms using a full-matrix least-squares method, the hydrogen atoms were placed in idealized positions and were held fixed during final anisotropic refinement of the non-hydrogen atoms. The final residuals were $R(F) = 0.058$ and $R_w(F) = 0.057$.

There were numerous peaks on the order of 1–2 e/Å^3 in the final difference map, probably due to the fact that the crystal was large and no absorption correction was made. Most of these were in the immediate vicinity of the heavy-atom (W_2Cl_7) group. The largest peak was 2.17 e/Å^3.

Acknowledgment. We wish to thank the National Science Foundation, Department of Energy, Office of Basic Research, Chemical Sciences Division, and the Wrubel Computing Center for support, B. K. Conroy and K. A. Stahl for experimental assistance, and Professor R. A. D. Wentworth for helpful discussions. We also thank the NSF for departmental instrumentation grants: CHE-81-11957, CHE-81-05004, CHE-83-09446 and CHE-84-05851, and CHE-77-09496.

Registry No. $NaW_2Cl_7(THF)_5$, 109764-48-9; $W_2(NMe_2)_6$, 54935-70-5; $W_2(O\text{-}t\text{-}Bu)_6$, 57125-20-9; $W_2(CH_2\text{-}t\text{-}Bu)_6$, 54453-68-8; W, 7440-33-7.

Supplementary Material Available: Stereoviews of the $NaW_2Cl_7(THF)_5$ molecule and tables of anisotropic thermal parameters and complete bond distances and angles (5 pages); a listing of observed and calculated structure factors (9 pages). Ordering information is given on any current masthead page.

---

(20) Chisholm, M. H.; Folting, K.; Huffman, J. C.; Kirkpatrick, C. C. *Inorg. Chem.* **1984**, *23*, 1021.

Contribution from the Institut für anorganische, analytische und physikalische Chemie, Universität Bern, CH-3000 Bern 9, Switzerland, and the Institut de Chimie, Université de Neuchâtel, CH-2000 Neuchâtel, Switzerland

Ferromagnetic Exchange Interaction in a Binuclear Chromium(III) Complex: Magnetic and Spectroscopic Properties of $[(H_2O)_4Cr(OH)_2Cr(H_2O)_4][(CH_3)_3C_6H_2SO_3]_4\cdot 4H_2O$

Christian Reber,[1a] Hans U. Güdel,*[1a] Leone Spiccia,[1b] and Werner Marty[1b]

Received March 20, 1987

The exchange interactions in $[(H_2O)_4Cr(OH)_2Cr(H_2O)_4][(CH_3)_3C_6H_2SO_3]_4\cdot 4H_2O$ have been investigated by polarized single-crystal absorption spectroscopy and powder magnetic susceptibility measurements. Within the binuclear complex unit the exchange is ferromagnetic with $J = 5.0$ cm^{-1}. A dehydrated sample showed much weaker ferromagnetic behavior ($J = 0.8$ cm^{-1}), indicating a strong dependence of the exchange interaction on small changes in molecular geometry. At temperatures below 5 K two-dimensional antiferromagnetic ordering sets in. The lowest energy absorption transitions gain intensity through a single-ion mechanism. Their energetic positions can be rationalized with a set of orbital exchange parameters confirming the overall ferromagnetic intradimer interaction.

1. Introduction

The study of exchange interactions in binuclear chromium(III) complexes has been an active field of research in recent years. Bis(μ-hydroxo)-bridged dimeric complexes represent an especially well investigated set of compounds.[2] Usually the exchange coupling within these binuclear molecular units turns out to be antiferromagnetic. For the ground state the well-known Heisenberg Hamiltonian (eq 1) gives an accurate description of the

---

(1) (a) Universität Bern. (b) Université de Neuchâtel.

(2) Hodgson, D. J. In *Magneto-Structural Correlations in Exchange Coupled Systems*; Willett, R. D., Gatteschi, D., Kahn, O., Eds.; D. Reidel: Dordrecht, The Netherlands, 1985; NATO ASI Series Vol. C140, and references therein.

$$H_{ex} = -2J\vec{S}_a \cdot \vec{S}_b \qquad (1)$$

experimentally observed energetic splittings. The magnitude of $-2J$ was found to vary from compound to compound despite the similar coordination in all these complexes. The observed $-2J$ values range from 0.6 cm^{-1} for $[(NH_3)_4Cr(OH)_2Cr(NH_3)_4]Br_4 \cdot 4H_2O$[3] on the one hand to 43 cm^{-1} for $[(1,10\text{-phen})_2Cr(OH)_2Cr(1,10\text{-phen})_2]Cl_4 \cdot 6H_2O$[4] (1,10-phen = 1,10-phenanthroline) on the other. As in these two examples, the majority of systems investigated so far contain nitrogen atoms coordinated to the chromium(III) ion in the nonbridging positions. There are fewer cases of oxygen-coordinated complexes, and most of these contain carboxylato groups as ligands.[5] Up to the present time, $Na_4[(mal)_2Cr(OH)_2Cr(mal)_2] \cdot 5H_2O$[6] (mal = malonato) is the only binuclear chromium(III) compound that has been reported to have a very small ferromagnetic exchange coupling. Here we present the first study of a binuclear complex coordinated only by H_2O, containing molecular $[(H_2O)_4Cr(OH)_2Cr(H_2O)_4]^{4+}$ units. The simple ligands and the very uniform first coordination sphere make the title compound an attractive model system for the study of the exchange interactions between the chromium(III) ions. Such a uniform oxygen environment is otherwise only found in systems that contain chromium(III) ions doped in oxide host lattices as for example Al_2O_3 (ruby) or $ZnGa_2O_4$[7] but not in molecular coordination compounds. The main advantage of a concentrated system lies in the fact that only one molecular species containing chromium(III) ions is present. In contrast, a doped crystal contains a variety of different chromium(III) units ranging from single ions and pairs to large clusters. This precludes the use of magnetic measurements, and it can make the analysis of spectroscopic results extremely difficult.

The title compound crystallizes in the monoclinic space group $P2_1/a$; the complete structure has been reported elsewhere.[8] The chromium(III) pairs are arranged in layers that are separated by two layers of mesitylene-2-sulfonate anions.

There is extensive hydrogen bonding between nearest-neighboring dimers in the layers involving both the crystal water molecules and the anion's sulfonato groups as intermediates.[8] This highly anisotropic structure leads to a pronounced anisotropy of physical properties. In particular, weak interdimer exchange is dominant within the layers, resulting in two-dimensional magnetic ordering at very low temperatures.

In the present paper, we use magnetic susceptibility and optical spectroscopy measurements to determine the nature of the exchange coupling within the title complex. The intradimer coupling is found to be ferromagnetic, thus giving rise to interdimer interactions at low temperatures, which are investigated by magnetic susceptibility measurements. From the energy splittings in the singly excited $^2E_g{}^4A_{2g}$ state, which are determined by absorption spectroscopy, orbital exchange parameters are estimated. They are consistent with the ferromagnetic coupling in the ground state.

2. Experimental Section

The preparation of the $[(H_2O)_4Cr(OH)_2Cr(H_2O)_4]((CH_3)_3C_6H_2SO_3)_4 \cdot 4H_2O$ complex is described in detail elsewhere.[8] Crystals suitable for spectroscopic measurements were prepared by dissolution of 1 g of complex in 10 mL of 0.02 M mesitylene-2-sulfonic acid (suppresses the hydrolysis of the complex) at ca. 60 °C followed by cooling to room temperature and, in some cases, seeding of the solution. Crystals of the required size and quality were obtained after several days. Their elemental and thermogravimetric analyses were as given in ref 8.

All the samples were further checked by powder X-ray diffraction with a Guinier–de Wolff camera using Cu $K\alpha_1$ radiation. The crystal system is monoclinic (space group $P2_1/a$) with the lattice constants a = 8.720 Å, b = 34.230 Å, c = 8.921 Å, and β = 96.59°.[8] There are two equivalent formula units per unit cell. The samples cleave easily perpendicular to the crystallographic b axis and show very clear extinction directions under a polarizing microscope. The orientation of the crystallographic a and c axes with respect to the macroscopic crystal edges was determined by single-crystal X-ray diffraction using a precession camera.[9]

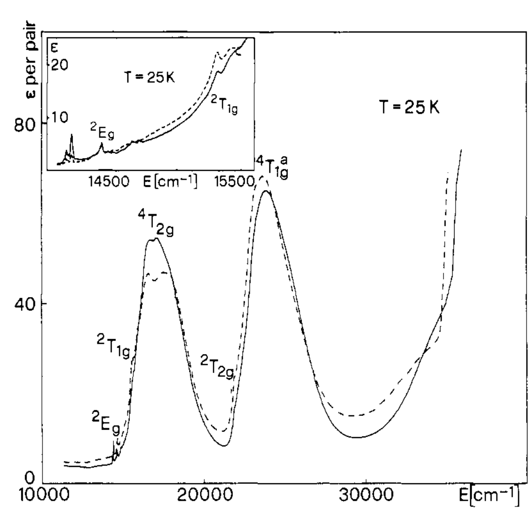

Figure 1. Polarized absorption spectra of $[(H_2O)_4Cr(OH)_2Cr(H_2O)_4][(CH_3)_3C_6H_2SO_3]_4 \cdot 4H_2O$ for light propagating parallel to the b axis (solid lines, $\vec{E} \parallel a$; dashed lines, $\vec{E} \perp a$). Band assignments are in O_h (single-ion designations). The insert shows the region of ^2E_g, $^2T_{1g}$ transitions in more detail.

Absorption spectra were recorded on a Cary 17 spectrophotometer equipped with a pair of Glan–Taylor prisms. The crystals were cooled in a closed-cycle helium cryostat (Air Products CSA-202G). Polarized transmission spectra with high resolution were recorded as follows: the light of a 100-W quartz halogen lamp (Oriel 6323) was dispersed by a 0.75-m monochromator (Spex 1702), polarized with a Rochon prism, and, after passing through the crystal, detected with a cooled photomultiplier (EMI 9659 QB), in conjunction with a tuning fork chopper and a lock-in amplifier (PAR 186A). The samples were cooled by means of the helium gas flow-tube technique[10] for temperatures above 10 K or with a helium-bath cryostat (Oxford Instruments MD4) for the 4.2 K spectra. Conversion of the transmission data to absorption as well as the data acquisition for the optical spectroscopic experiments was performed with a microcomputer (Tektronix 4052A).

The magnetic susceptibilities were measured at ETH Zürich with the moving-sample technique. For the measurements the magnetic field was chosen such that the magnetization depended linearly on the field strength. The resulting susceptibility values were corrected for diamagnetism by using the tabulated values for the atoms.[11] The powder susceptibility of the title compound as well as a dehydrated sample was obtained. The latter was prepared by keeping a powder of $[(H_2O)_4Cr(OH)_2Cr(H_2O)_4][(CH_3)_3C_6H_2SO_3]_4 \cdot 4H_2O$ at 90 °C for 12 h. According to the thermogravimetric results of ref 8 this corresponds to the loss of all four noncoordinated water molecules of the formula unit. The X-ray pattern of a powdered sample of the tetrahydrate was found to be in good agreement with a LAZY PULVERIX calculation,[12] indicating no preferred orientation of the crystallites.

3. Results

Polarized low-temperature absorption spectra of the title compound are shown in Figure 1. The main features can be rationalized in terms of an octahedrally coordinated single chromium(III) ion. Thus, in Figure 1 the final states of the transitions are labeled in O_h notation. The shape of the two spin-allowed absorption bands clearly indicates a superposition of more than one transition. A splitting of both $^4T_{2g}$ and $^4T_{1g}$ into three orbital components as a result of the local point symmetry (C_1) is expected. In the related $[(en)_2Cr(OH)_2Cr(en)_2]^{4+}$ complex this

---

(3) Decurtins, S.; Güdel, H. U. *Inorg. Chem.* **1982**, *21*, 3598.

(4) Glerup, J.; Hodgson, D. J.; Pedersen, E. *Acta Chem. Scand., Ser. A* **1983**, *A37*, 161.

(5) Scaringe, R. P.; Hatfield, W. E.; Hodgson, D. J. *Inorg. Chim. Acta* **1977**, *22*, 175.

(6) Scaringe, R. P.; Hatfield, W. E.; Hodgson, D. J. *Inorg. Chem.* **1977**, *16*, 1600.

(7) van Gorkom, G. G. P.; Henning, J. C. M.; van Stapele, R. P. *Phys. Rev. B: Condens. Matter* **1973**, *8*, 955.

(8) Spiccia, L.; Stoeckli-Evans, H.; Marty, W.; Giovanoli, R. *Inorg. Chem.* **1987**, *26*, 474.

(9) Stoeckli-Evans, H., private communication.

(10) Ferguson, J. In *Electronic States of Inorganic Compounds: New Experimental Techniques*; Day, P., Ed.; D. Reidel: Dordrecht, The Netherlands, 1975.

(11) Landolt-Börnstein, *Numerical Data and Functional Relationships in Science and Technology*; New Series, Hellwege, K.-H., Ed.; Springer-Verlag: West Berlin, 1976; New Series, Vol. II/8, p 27.

(12) Yvon, K.; Jeitschko, W.; Parthé, E. *J. Appl. Crystallogr.* **1977**, *10*, 73.

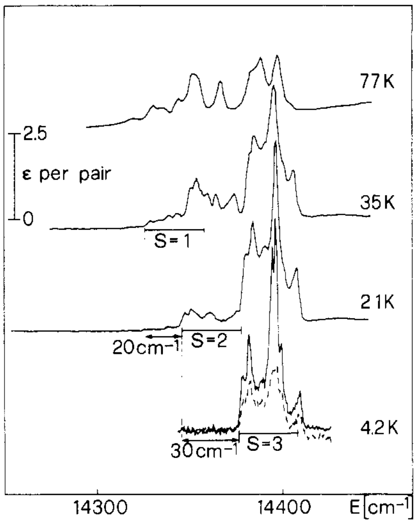

Figure 2. Detailed absorption spectra of the $^4A_{2g}{}^4A_{2g} \rightarrow {}^4A_{2g}{}^2E_g$ electronic origins for light propagating parallel to the *b* axis and $E \parallel a$. For each group of transitions the total spin quantum number *S* of the initial state is given. The energetic separation of the band systems is indicated below the arrows. For the lowest temperature both polarizations are shown (dashed line, $E \perp a$).

splitting was found to be fully resolved and larger than in the title complex. The ^2E_g and $^2T_{1g}$ transitions are both very close in energy to the first spin-allowed ($^4T_{2g}$) absorption. This is in contrast to the case for nitrogen-coordinated chromium(III) ions, where the separation is larger due to the stronger ligand field caused by the nitrogen ligator atoms.[13] In the 25 K spectrum it is even possible to identify the $^2T_{2g}$ transitions. A very interesting feature of the absorption spectrum (Figure 1) is the *absence* of sharp lines in the near-UV region, which would correspond to the simultaneous excitation of both chromium(III) ions to ^2E_g, $^2T_{1g}$, or $^2T_{2g}$. This is the first binuclear chromium(III) complex measured in our laboratory that does not show these double-excitation bands so typical of exchange-coupled compounds.

The lowest energy absorption bands corresponding to $^2E_g{}^4A_{2g}$ single excitations are shown at various temperatures and under high resolution in Figure 2. There are clearly three sets of bands with distinct temperature behavior, which are discussed in parts 4.1 and 4.3.

Despite many careful attempts, we were not able to obtain genuine luminescence spectra of the title compound. Weak luminescence was observed from all the samples studied, but the observed sample dependence pointed to an impurity origin. This was confirmed by selective excitation experiments with a dye laser, which clearly established the absence of any intrinsic luminescence down to 1.5 K. The nonradiative deactivation obviously dominates the radiative pathway completely even at the lowest temperatures. High-energy O–H stretching vibrations are well-known as efficient accepting modes, much more efficient than for instance N–H vibrations. Recently a series of H_2O- and NH_3-coordinated octahedral chromium(III) complexes was prepared and spectroscopically investigated.[14] The luminescence quantum yield as well as the decay time decreased significantly upon increasing the number of H_2O ligands from 0 to 6. In our binuclear complex the excitation is delocalized over both chromium(III) centers and we have 18 OH groups in the first coordination sphere compared to the maximum of 12 groups in a mononuclear complex. Thus, it is plausible that no luminescence could be observed from the title compound. This very powerful method, which often directly yields the ground-state exchange splittings in chromium(III) pairs, was therefore not applicable in the present case. In Figure 3 the magnetic susceptibility measurements are shown as $\chi_M T$ vs. *T* curves. Here we investigated the title compound as well as a dehydrated sample. The ferromagnetic nature of the intradimer exchange coupling is apparent at first sight, even without any deep analysis, from the increase of $\chi_M T$ at low temperatures. The model fits shown in the inserts are discussed in parts 4.1 (dashed lines) and 4.2 (solid lines), respectively.

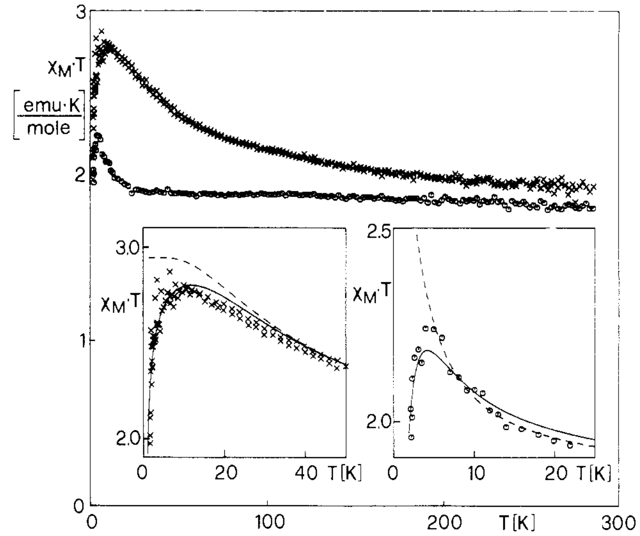

Figure 3. Temperature dependence of $\chi_M T$ per Cr^{3+} ($\chi_M T = 0.125\mu_{eff}^2$). Experimental values for $[(H_2O)_4Cr(OH)_2Cr(H_2O)_4][(CH_3)_3C_6H_2SO_3]_4{\cdot}4H_2O$ are shown as crosses; circles represent the measurements for the dehydrated compound. The inserts show model fits to the data. Dashed and solid lines correspond to eq 1 and 3, respectively.

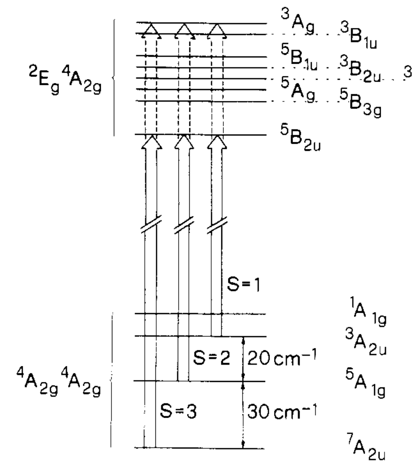

Figure 4. Experimentally determined ground-state splitting and calculated splitting of the first excited state from the parameters of eq 5. The pair levels are designated in D_{2h} notation. The solid and dashed arrows indicate the spectral ranges of absorption for the three sets of bands designated as $S = 3$, $S = 2$, and $S = 1$ in Figure 2.

4. Analysis and Discussion

4.1. Ground-State Properties: Intradimer Exchange. The ground-state magnetic moment of chromium(III) is spin-only to a good approximation. A Heisenberg operator (eq 1) therefore provides an adequate description of the exchange interactions in a binuclear complex.

The resulting splitting corresponds to a Landé pattern with *S*, the dimer spin quantum number, ranging from 0 to 3. For positive *J*, i.e. ferromagnetic coupling, we obtain the pattern shown in Figure 4. The orbital designation of the pair levels in Figure 4 is based on the idealized D_{2h} dimer symmetry.[3] The actual dimer symmetry is C_i.

The observed rise of $\chi_M T$ above 1.84 emu K mol⁻¹ on lowering of the temperature (Figure 3) is a clear indication of ferromagnetic intradimer coupling. Both the tetrahydrate and the dehydrated compound show the same qualitative behavior, but in the latter the rise occurs at lower temperatures. The strength of the ferromagnetic coupling is obviously greater in the tetrahydrate. A numerical value of *J* is obtained by fitting the eigenvalues of eq

---

[13] Chatterjee, K. K.; Forster, L. S. *Spectrochim. Acta* **1964**, *20*, 1603.
[14] Mvele, M.; Wasgestian, F. *Spectrochim. Acta, Part A* **1986**, *42A*, 775.

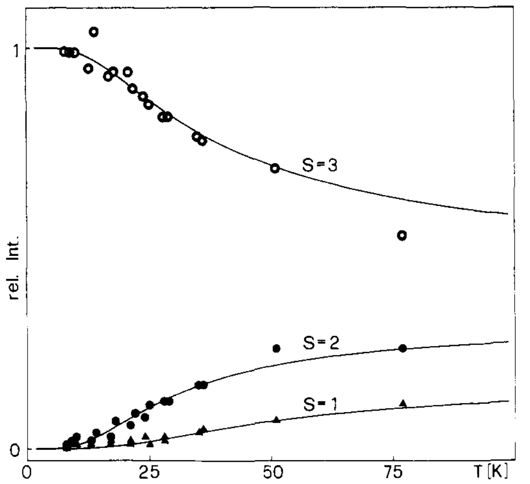

Figure 5. Absorption intensity of the $^4A_{2g}{}^4A_{2g} \rightarrow {}^4A_{2g}{}^2E_g$ electronic origins as a function of temperature. The experimental points for the three band systems designated as $S = 1$, $S = 2$, and $S = 3$ in Figure 2 are given as ▲, ●, and ○, respectively. Due to the overlap of the band systems at higher temperatures, the estimated experimental error approaches 20% at 77 K. The solid lines are fits to the Boltzmann population of the ground-state pair levels as discussed in part 4.1.

1 with their magnetic moments to the observed $\chi_M T$ values above 25 and 7 K for the tetrahydrate and the dehydrated compound, respectively. When g is set to 1.98, this is a one-parameter fit and we get $J_{\text{tetrahydrate}} = 4.8 \pm 0.2$ cm^{-1} and $J_{\text{dehydrated}} = 0.8 \pm 0.2$ cm^{-1}. The corresponding calculated curves are shown as broken lines in Figure 3.

The absorption spectra in Figure 2 allow an independent determination of the ground-state splitting for the tetrahydrate. The observed transition energies can be used as well as the temperature dependence of intensities.

We can distinguish three slightly overlapping band systems with distinctly different temperature dependences. They are designated $S = 3$, $S = 2$, and $S = 1$ in Figure 2. At 4.2 K the $^4A_{2g}{}^4A_{2g} \rightarrow {}^2E_g{}^4A_{2g}$ pair excitations span an energy range of only 31 cm^{-1} (band system $S = 3$). These bands lose intensity with increasing temperature, and at the same time the hot band systems $S = 2$ and $S = 1$ arise at lower energy. Figure 5 shows a plot of the experimental intensities vs. temperature and the result of a one-parameter fit of the Boltzmann populations within the pair spin levels. $J = 5.2 \pm 0.3$ cm^{-1} is obtained, in very good agreement with the magnetochemical value.

The energy shifts between the band systems $S = 3$ and $S = 2$ and between $S = 2$ and $S = 1$ in Figure 2 are 30 and 20 cm^{-1}, respectively. If we assume a situation as depicted in Figure 4, i.e. transitions to all the levels of the $^2E_g{}^4A_{2g}$ excited state, then the above shifts correspond to the energy differences between the $S = 3$, 2, and 1 ground levels: $4J = 20$ cm^{-1} and $6J = 30$ cm^{-1}. The resulting $J = 5$ cm^{-1} is again in excellent agreement with the above values.

Taking the average of the three J values for the tetrahydrate and the magnetochemical result for the dehydrated compound, we thus obtain

$$\begin{aligned} J_{\text{tetrahydrate}} &= 5.0 \pm 0.2 \text{ cm}^{-1} \\ J_{\text{dehydrated}} &= 0.8 \pm 0.2 \text{ cm}^{-1} \end{aligned} \tag{2}$$

How can we account for the ferromagnetic nature of J and the different values in the two compounds? Of the bis(μ-hydroxo)-bridged dinuclear chromium(III) complexes described in the literature all but one are antiferromagnetically coupled. The one exception is $Na_4[(mal)_2Cr(OH)_2Cr(mal)_2]\cdot 5H_2O$,[6] with a J value of 1.08 cm^{-1}, very similar to the value for our dehydrated compound. Encouraged by the beautiful correlation between J and the bridging angle in analogous copper(II) complexes,[15] various researchers have attempted to correlate magnetic and structural properties also in bis(μ-hydroxo)-bridged chromium(III) complexes.[4,16–18] They show that the situation is much more complicated than for copper(II). The most convincing attempt at correlating structural data and J values for a very large number of chromium(III) diols is perhaps that given in ref 4. Besides the distances and angles within the

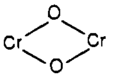

group, the tilting angle α of the O–H bond out of the CrOCr plane was found to be an important parameter. This was independently confirmed by a detailed optical spectroscopic study of $[(en)_2Cr(OH)_2Cr(en)_2]Br_4\cdot 2H_2O$[3] and $[(NH_3)_4Cr(OH)_2Cr(NH_3)_4]Cl_4\cdot 4H_2O$,[3] in which the orbital exchange parameters constituting the overall parameter J were determined. It was found that the out-of-plane interaction involving the p_z orbital on the bridging oxygen was the dominant pathway for antiferromagnetic exchange. For large tilting angles α this pathway is disrupted because the p_z orbital on oxygen participates in σ bonding.

In the title compound, the bridging OH groups are involved in hydrogen bonds with the sulfonate groups of the anions. Taking the crystallographically estimated position of the H atom, we obtain a value of 43° for the tilting angle. With this and the other relevant parameters, i.e. the Cr–O_{bridge}–Cr angle of 101.8° and the Cr–O_{bridge} distance of 1.936 Å, we calculate $-2J = 18.5$ cm^{-1} by using the model of ref 4. The discrepancy between this value and our experimentally observed $-2J = -10.0$ cm^{-1} is much larger than in any of the examples of ref 4.

Upon dehydration the layer structure of the tetrahydrate is essentially retained, as is shown by the presence of the dominant reflection in the X-ray powder pattern at $d = 17.12$ Å corresponding to the distance between the magnetic layers. By the removal of the water molecules the hydrogen-bonding network within the layers is destroyed, leading to a rearrangement of the dinuclear chromium(III) complexes. We ascribe the different J values of the hydrated and dehydrated salts to differences in the packing of the dinuclear complexes, which are likely to lead to different angles α.

The exchange parameter J can be considered as being composed of ferromagnetic and antiferromagnetic parts. The ferromagnetic parts are very hard to estimate theoretically. The antiferromagnetic parts corresponding to kinetic exchange[19] can be correlated with energy differences between molecular orbitals arising from the magnetic atomic orbitals. Approximate calculations of such energy differences are able to account for a trend in the antiferromagnetic part of the exchange interaction within a series of similar compounds. Kahn et al. have performed extended Hückel calculations for oxygen-coordinated chromium(III) pairs similar to our complex.[17] They found a minimum of the antiferromagnetic contribution at a Cr–O–Cr angle of 102°, very close to the angle of 101.8° in the title compound. Although they did not consider the tilting angle of the hydrogen atom defined above, this result is in good agreement with the ferromagnetic nature of our complex.

4.2. Ground-State Properties: Interdimer Exchange. The observed drop of $\chi_M T$ below 10 K indicates some kind of antiferromagnetic effect. There is no sharp discontinuity in the $\chi_M T$ vs. T curve, which would indicate a transition to a three-dimensionally ordered magnetic phase. The smooth variation of $\chi_M T$ vs. T observed in both the tetrahydrate and the dehydrated salt indicates the onset of magnetic ordering between the dimeric complexes in one or two dimensions. The tetrahydrate has a pronounced layer structure with neighboring magnetic layers separated along the b axis by a double layer of bulky anions. The nearest Cr–Cr distance between the layers is 18.1 Å. Within the layers a given complex has two types of neighbors. The corre-

---

(15) Crawford, V. H.; Richardson, H. W.; Wasson, J. R.; Hodgson, D. J.; Hatfield, W. E. *Inorg. Chem.* **1976**, *15*, 2107.

(16) Kahn, O.; Briat, B. *J. Chem. Soc., Faraday Trans. 2* **1976**, *72*, 268.

(17) Charlot, M. F.; Kahn, O.; Drillon, M. *Chem. Phys.* **1982**, *70*, 177.

(18) Hodgson, D. J. *ACS Symp. Ser.* **1974**, *No. 5*, 94.

(19) Anderson, P. W. *Solid State Phys.* **1963**, *14*, 99.

sponding Cr–Cr separations are 8.7 and 11.7 Å. In a projection on the *ac* plane they are approximately parallel to *a* and are along the bisection of β, respectively. The intermolecular connection along the *a* axis involves sulfonate groups of the anions in the manner

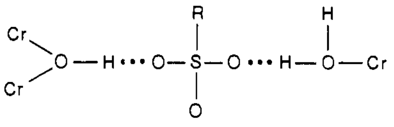

I

whereas the connection along the bisection of β involves hydrogen bonds of the type

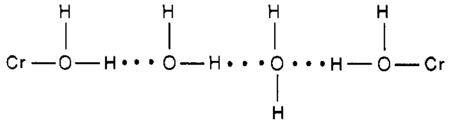

II

Both of these connections provide possible pathways for weak intermolecular interactions, and we therefore consider the tetrahydrate as a two-dimensional system. After dehydration, hydrogen bonding within the magnetic layers is only possible through the anion sulfonate groups. Since we do not know the connectivity in this structure, it can be either a one- or a two-dimensional magnetic system. In analogy to the case for the tetrahydrate it will be treated as two-dimensional in the following analysis. The dimer levels are assumed to be isotropic, and thus the interdimer exchange can be described by a Heisenberg Hamiltonian. Two-dimensional Heisenberg antiferromagnets have been investigated theoretically.[20] If we consider the two pathways discussed above in I and II as equivalent, the magnetic layers in the tetrahydrate correspond to a square lattice. Our two-dimensional system is a peculiar case since every constituent dimeric complex can have a spin *S* of 3, 2, 1, or 0. Therefore, a model calculation as described in ref 20 has to be modified by taking into account the Boltzmann population among the various *S* values. We neglected interactions between binuclear units with different *S* values and made the assumption that *J'*, the interdimer exchange parameter, is the same for every *S*. The resulting equation (eq 3)

$$\chi T = Ng^2\mu_B{}^2T(-2J')^{-1}\sum_{S=1}^{3}B(S)\cdot E(S) \tag{3}$$

$$E(S) = \left(3\theta + \sum_{n=1}^{\infty}\frac{C_n}{\theta^{n-1}}\right)^{-1}$$

$$B(S) = \frac{(2S+1)e^{-(12-S(S+1))J/kT}}{7 + 5e^{-6J/kT} + 3e^{-10J/kT} + e^{-12J/kT}}$$

$$\theta = kT(2|J'|S(S+1))^{-1}$$

was then fitted to our experimental χT vs. *T* data. C_n values are numerical coefficients tabulated for $n = 1$–6 in ref 20. With *g* fixed at 1.98 and *J* at the value given in eq 2, the only parameter to be fitted is *J'*. The results of these one-parameter fits are given as solid lines in Figure 3. In view of the assumptions made to obtain eq 3, the fits are excellent. The values for the interdimer exchange parameter *J'* are −0.010 ± 0.003 and −0.034 ± 0.004 cm^{-1} for the tetrahydrate and the dehydrated compound, respectively. The order of magnitude of the parameters *J'* appears reasonable for the exchange pathways I and II. In ref 6 a molecular field approach was chosen, in contrast to our analysis, to account for the antiferromagnetic behavior at the lowest temperatures. But since the structure of the title compound is distinctly two-dimensional, the model applied above is physically more appropriate to the present case. It is interesting to note that the ferromagnetic nature of the intradimer exchange enables the interdimer exchange to become manifest between 1.6 and 10 K. With the exception of $Cs_3Cr_2X_9$ (X = Cl, Br, I)[21] all other known chromium(III) compounds containing dinuclear complexes become nonmagnetic at low temperatures as a result of the antiferromagnetic intradimer exchange. In the ionic lattices $Cs_3Cr_2X_9$ (X = Cl, Br, I) at very low temperatures interdimer exchange can compete with intradimer exchange despite its antiferromagnetic nature.

4.3. Electronically Excited States. Energy splittings due to exchange interactions in the first excited state $^2E_g{}^4A_{2g}$ of chromium(III) dimers are usually well described by the effective Hamiltonian

$$H_{ex}' = -2\sum_{ij}J_{a_ib_j}(\vec{s}_{a_i}\cdot\vec{s}_{b_j}) \tag{4}$$

where *i* and *j* number the singly occupied t_{2g} orbitals. $J_{a_ib_j}$ values are orbital exchange parameters, the number of which is reduced from nine by the symmetry of the dimer. For a D_{2h} dimer there are four independent parameters, as outlined in detail in ref 3.

Electronic transitions that are spin-forbidden on the single ion can attain intensity through either spin–orbit coupling[22] or an exchange intensity mechanism.[23] The latter leads to the selection rule $\Delta S = 0$, whereas the former allows both $\Delta S = 0$ and $\Delta S = \pm 1$ dimer transitions.

Turning to the experimental results, we notice in Figure 2 that the total intensity of the absorptions near 14 400 cm^{-1} is essentially temperature-independent. Furthermore, we note in Figure 1 the absence of any double excitations in the near-UV region. Both of these observations are conspicuously different in behavior from the case for other dinuclear chromium(III) complexes such as $[(NH_3)_5Cr(OH)Cr(NH_3)_5]^{5+}$[24] and $[(en)_2Cr(OH)_2Cr(en)_2]^{4+}$.[3] We conclude that there is no exchange-induced absorption intensity in our complex. This is understandable and is related to the ferromagnetic coupling in the ground state. There is obviously a lack of orbital pathways for both antiferromagnetic exchange and exchange-induced intensity. Both of these can be related to the same electron-transfer integrals, which must be very small in our complex.

Another feature of the 4.2 K absorption spectrum that is distinctly different from the spectra of other dinuclear chromium(III) complexes is the very narrow range of 31 cm^{-1} of the 14 400-cm^{-1} absorption. In the related bis(μ-hydroxo)-bridged complexes $[(NH_3)_4Cr(OH)_2Cr(NH_3)_4]Cl_4\cdot 4H_2O$[3] and $[(en)_2Cr(OH)_2Cr(en)_2]Br_4\cdot 2H_2O$[3] the corresponding ranges are 180 and 505 cm^{-1}, respectively.

We conclude that the total spread of the dimer levels in the singly excited $^2E_g{}^4A_{2g}$ state is only 31 cm^{-1}, again as a result of very small or vanishing orbital parameters contributing to the splitting according to eq 4. Using the notation of ref 3 and the orbital exchange parameters of $[(NH_3)_4Cr(OH)_2Cr(NH_3)_4]Cl_4\cdot 4H_2O$ and $[(en)_2Cr(OH)_2Cr(en)_2]Br_4\cdot 2H_2O$[3] as a reference, we can make the following estimate of parameters for the title compound:

$$\left.\begin{array}{l} J_{xz\,xz} = J_{yz\,yz} \\ J_{yz\,xy} = J_{xy\,yz} = J_{xz\,xy} = J_{xy\,xz} \end{array}\right\} = 7.5\ \text{cm}^{-1}$$
$$\left.\begin{array}{l} J_{yz\,xz} = J_{xz\,yz} \\ J_{xy\,xy} \end{array}\right\} = 0\ \text{cm}^{-1} \tag{5}$$
$$\Delta E(^2A_1 - {}^2B_1) = 20\ \text{cm}^{-1}$$

The *z* axis is perpendicular to the

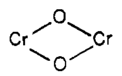

plane, and the *x* and *y* axes are approximately parallel to the Cr–O

---

(20) Lines, M. E. *J. Phys. Chem. Solids* **1970**, *31*, 101.

(21) Leuenberger, B.; Güdel, H. U.; Kjems, J. K.; Petitgrand, D. *Inorg. Chem.* **1985**, *24*, 1035.

(22) Namba, K.; Tanabe, Y. *J. Phys. Soc. Jpn.* **1974**, *37*, 371.

(23) Ferguson, J.; Guggenheim, H. J.; Tanabe, Y. *J. Phys. Soc. Jpn.* **1966**, *21*, 692.

(24) Riesen, H.; Güdel, H. U. *Mol. Phys.* **1986**, *58*, 509.

directions. In deriving (5), we have set equal to zero $J_{xz\,yz}$ and $J_{xy\,xy}$, the two antiferromagnetic parameters that dominate the picture in $[(en)_2Cr(OH)_2Cr(en)_2]Br_4{\cdot}2H_2O$[3] and $[(NH_3)_4Cr(OH)_2Cr(NH_3)_4]Cl_4{\cdot}4H_2O$.[3] The two ferromagnetic parameters $J_{xz\,yz}$ and $J_{xz\,xy}$ have magnitudes similar to those in the systems studied in ref 3. With the parameters in (5) the total energy splitting of the $^2E_g{}^4A_{2g}$ final states is calculated as 50 cm^{-1}, in fair agreement with the experimentally observed spread of 31 cm^{-1} at 4.2 K. The calculated excited-state levels are shown in Figure 4 with the observed transitions (Figure 2) indicated schematically as arrows. An independent check of these parameter values is based on the relationship

$$J = \tfrac{1}{9}\sum_{ij} J_{a_i b_j} \qquad (6)$$

We obtain the value $J = 5$ cm^{-1}, in exact agreement with the ground-state exchange parameter. This is reasonable because both $^4A_{2g}$ and ^2E_g are derived from the same electron configuration. We feel, therefore, that the above orbital parameters are meaningful, because they lead to a consistent picture not only for the title compound but also in comparison with other bis(μ-hydroxo)-bridged chromium(III) complexes.

Assignments of individual absorption bands to the $^2E_g{}^4A_{2g}$ dimer levels cannot be made with any confidence. We notice that the number of overlapping bands in the 14 400-cm^{-1} system exceeds the allowed ($\Delta S = 1$) four at 4.2 K. Since all the intensity in this spectral range is probably due to electronic origins, there must be $\Delta S = 2$ transitions contributing to the intensity. Weak $\Delta S = 2$ transitions have also been observed in $[(en)_2Cr(OH)_2Cr(en)_2]Br_4{\cdot}2H_2O$.[3] Deviations from the theoretically assumed isotropy of the dimer levels are most likely to be responsible for this.

Acknowledgment. We thank K. Mattenberger for performing the susceptibility measurements. Financial support of this work by the Swiss National Science Foundation is acknowledged.

Registry No. $[(H_2O)_4Cr(OH)_2Cr(H_2O)_4][(CH_3)_3C_6H_2SO_3]_4{\cdot}4H_2O$, 106402-71-5.

Contribution from Corporate Research and Development,
General Electric Company, Schenectady, New York 12301

Single-Crystal X-ray Structure of the High-Temperature Superconductor $Ba_2YCu_3O_{7-x}$

M. F. Garbauskas,* R. H. Arendt, and J. S. Kasper

Received July 2, 1987

We have determined the crystal structure of the high-temperature superconductor $Ba_2YCu_3O_{7-x}$ by single-crystal X-ray diffraction techniques. This material, which has a critical temperature of about 90 K, is orthorhombic with lattice parameters $a = 3.829$ (1), $b = 3.886$ (1), and $c = 11.694$ (3) Å, for space group *Pmmm*, $Z = 1$. The structure is a variant of the simple perovskite arrangement with an ordering of the Ba and Y cations. In the layers normal to the *c* axis there is a total absence of oxygen for those containing Y cations, while there is an oxygen vacancy and a partially occupied oxygen site in the Cu layer between the Ba layers. A specimen of apparent tetragonal symmetry was also studied, but the tetragonality, in that case, was the result of twinning of the orthorhombic structure.

Introduction

The structure of $Ba_2YCu_3O_{7-x}$ has been a matter of great interest and considerable discussion, since it was reported that this material exhibited superconductivity at approximately 90 K. The general picture of a layered variant of perovskite has been proposed by several investigators, although there seems to be some confusion regarding the details of the structure, especially the positions and occupancy of the oxygen sites. The high-resolution neutron powder diffraction work of Beno et al.[1] described an orthorhombic cell similar to that presented here. There have been other reports, however, of another orthorhombic cell[2] and of a tetragonal structure.[3] In this paper, we report two single-crystal studies: one is for the orthorhombic single crystal; the other deals with what appeared to be a tetragonal single crystal, but which we now believe to be a twinned orthorhombic crystal, with (110) as the twin plane.

Experimental Section

Reagent grade $BaCO_3$ (J. T. Baker), Y_2O_3 (Research Chemicals, 99.9% pure), and CuO, GR grade (EM Science, analyzed by H_2 reduction as 99.9% CuO), were weighed out in the 2:1:3 cation ratio. The mixture was wet-milled for 3 h in a polyethylene jar with dense ($^3/_8$ in. diameter) zirconia media in water containing a small amount of Triton X-100 wetting agent. The milled mixture was oven dried at 120 °C overnight. The dried material was reacted by heating at 100 °C/h to 950 °C and holding for 24 h, followed by furnace cooling at <150 °C/h to room temperature. The reaction was carried out in an ambient air atmosphere with the powder bed less than a centimeter in depth. The product was gently crushed in a porcelain mortar and pestle. Small irregularly shaped single crystals were identified and isolated in a sample of this black material.

Table I. Atom Coordinates (×10^4) and Temperature Factors (Å^2 × 10^3) for the Tetragonal Crystal in $P\bar{4}2m$

atom	x	y	z	$U_{\text{equiv}}{}^a$	occupancy
Cu(1)	0	0	0	23 (1)	1.00
Cu(2)	0	0	3556 (2)	21 (1)	1.00
Y	5000	5000	5000	20 (1)	1.00
Ba	5000	5000	1849 (1)	22 (1)	1.00
O(1)	5000	0	0	28 (8)	0.40
O(2)	0	0	1538 (7)	29 (2)	1.00
O(3)	5000	0	3782 (5)	20 (2)	1.00

^{a} Equivalent isotropic U defined as one-third of the trace of the orthogonalized $\mathbf{U}_{ij}$ tensor.

For both structures, single-crystal data were collected by using a Nicolet P3F automated single-crystal diffractometer and monochromatized Mo Kα radiation ($\lambda = 0.710\,69$ Å) at room temperature. An $\omega/2\theta$ scan was used to collect an entire sphere of data ($\pm h,\pm k,\pm l$) from 4 to 50° in 2θ. Since the crystals were very irregular, indices could not be assigned to the faces. Therefore, an empirical absorption correction was applied to the data for each crystal ($\mu = 293.4$ cm^{-1}; $\mu r = 2.0$). The materials were known to be perovskites, and therefore, atomic positions were assigned based on this structure and refined by using the SHELXTL program package.[4] All atoms were treated as anisotropic, and the occupancies of the oxygen atoms were allowed to refine. The function minimized in least-squares refinement is $\sum w(|F_o| - |F_c|)^2 \cdot R = \sum ||F_o| - |F_c|| / \sum |F_o|$.

Powder diffraction data were collected by using a Siemens D500 automated diffractometer using Cu Kα radiation. Powder patterns were

---

(1) Beno, M. A.; Soderholm, L.; Capone, D. W.; Hinks, D. G.; Jorgensen, J. D.; Schuller, I. K.; Segre, C. U.; Zhang, K.; Grace, J. D., submitted for publication in *Appl. Phys. Lett.*

(2) Siegrist, T.; Sunshine, S.; Murphy, D. W.; Cava, R. J.; Zahurak, S. M. *Phys. Rev. B: Condens. Matter* **1987**, *35*, 7137.

(3) Hazen, R. M.; Finger, L. W.; Angel, R. J.; Prewitt, C. T.; Ross, N. L.; Mao, H. K.; Hadidiacos, C. G.; Hor, P. H.; Meng, R. L.; Chu, C. W. *Phys. Rev. B: Condens. Matter* **1987**, *35*, 7238.

(4) Sheldrick, G. M. "SHELXTL", Nicolet Instrument Corp.: Madison, WI, 1983. Scattering factors from: *International Tables for X-ray Crystallography*; Kynoch: Birmingham, England, 1974; Vol. 4 pp 55-60, 99-101, 149-150.